The involvement of $Ca_v3.2/\alpha_{1H}$ T-type calcium channels in excitability of mouse embryonic primary vestibular neurones

Laurence Autret[1], Ilana Mechaly[1], Frédérique Scamps[1], Jean Valmier[1], Philippe Lory[2] and Gilles Desmadryl[1]

[1] *Institut des Neurosciences de Montpellier, INSERM U583, Hôpital Saint Eloi, 80 rue Augustin Fliche, 34091 Montpellier cedex 5, France*
[2] *Institut de Génomique Fonctionnelle, CNRS UMR 5203, INSERM U661, 141 rue de la Cardonille, 34094 Montpellier cedex 5, France*

Ca^{2+} influx through voltage-gated calcium channels probably influences neuronal ontogenesis. Many developing neurones transiently express T-type/Ca_v3 calcium channels that contribute to their electrical activity and potentially to their morphological differentiation. Here we have characterized the electrophysiological properties and the functional role of a large T-type calcium current that is present in mouse developing primary vestibular neurones at embryonic day E17. This T-type current showed fast activation and inactivation, as well as slow deactivation kinetics. The overlap of activation and inactivation parameters produced a window current between −65 and −45 mV. Recovery from short-term inactivation was slow suggesting the presence of the $Ca_v3.2$ subunit. This T-type current was blocked by micromolar concentrations of Ni^{2+} and was inhibited by fast perfusion velocities in a similar fashion to recombinant $Ca_v3.2$ T-type channels expressed in HEK-293 cells. More importantly, current clamp experiments have revealed that the T-current could elicit afterdepolarization potentials during the repolarization phase of action potentials, and occasionally generate calcium spikes. Taken together, we demonstrate that the $Ca_v3.2$ subunit is likely to be the main T-type calcium channel subunit expressed in embryonic vestibular neurones and should play a key role in the excitability of these neurones during the ontogenesis of vestibular afferentation.

(Resubmitted 26 April 2005; accepted after revision 15 June 2005; first published online 16 June 2005)
Corresponding author G. Desmadryl: INSERM U583, INM, Hôpital Saint Eloi, 80 rue Augustin Fliche, 34091 Montpellier cedex 5, France. Email: desmad@univ-montp2.fr

During early neuronal differentiation, Ca^{2+} entries play a critical role in axon outgrowth, growth cone motility (Spitzer *et al.* 2000*a*) and neuronal excitability (Spitzer *et al.* 2000*b*; Martin-Caraballo & Greer, 2001). It is recognized that voltage-gated calcium channels participate in this Ca^{2+} influx (McCobb *et al.* 1989; Thompson & Wong, 1991; Lorenzon & Foehring, 1995) and contribute to neuronal differentiation (Desarmenien & Spitzer, 1991; Gu & Spitzer, 1995; Tang *et al.* 2003). Because they are expressed at the early stages of neuronal development, T-type, low-voltage-activated (LVA) calcium channels (T-channels) have long been shown to play a crucial role in neuronal differentiation (Yaari *et al.* 1987; McCobb *et al.* 1989; Thompson & Wong, 1991; Desarmenien *et al.* 1993).

To date, three different T-channel subunit isoforms, designated as $Ca_v3.1/\alpha_{1G}$, $Ca_v3.2/\alpha_{1H}$ and $Ca_v3.3/\alpha_{1I}$, have been cloned and characterized (Cribbs *et al.* 1998; Perez-Reyes *et al.* 1998; Lee *et al.* 1999*a*; Monteil *et al.* 2000*a*,*b*). These subunits vary in their electrophysiological properties such as activation, inactivation and deactivation kinetics, as well as recovery properties following short-term inactivation (Klockner *et al.* 1999; Lee *et al.* 1999*a*; McRory *et al.* 2001*a*,*b*; Chemin *et al.* 2002*a*). These isotypes also display distinct sensitivity to Ni^{2+} (Lee *et al.* 1999*b*), show differences in their distribution in the nervous system (Talley *et al.* 1999) and, as expected, differ in their roles in physiology (for review see Perez-Reyes, 2003). Further, $Ca_v3.2$ subunit expression has been correlated with skeletal muscle (Bijlenga *et al.* 2000) and neuronal (Chemin *et al.* 2002*b*; Mariot *et al.* 2002) differentiation.

In the mouse embryonic peripheral vestibular system, large T-type calcium currents (T-currents) were recorded in neurones isolated between embryonic day 14 (E14) and E17 (Chambard *et al.* 1999). The proportion of neurones with a large T-current decreased drastically between E17 and postnatal day 4 (P4) (Desmadryl *et al.* 1997; Chambard *et al.* 1999). This change in T-channel expression coincides

 DOI: 10.1113/jphysiol.2005.089342

with the neurite outgrowth which starts at E13 and E14 and reaches a maximum around E17 (Nordemar, 1983), when the first synaptic contacts with the sensory cells are observed (Anniko, 1983; Mbiene *et al.* 1988; Desmadryl & Sans, 1990). Because the presence of a large T-current at E17 is transient and occurs at a critical period of the development and maturation of vestibular neurones, we have analysed its properties and function in acutely isolated E17 vestibular neurones. Here, we demonstrate that their electrophysiological and pharmacological properties are similar to those of the T-current generated by the recombinant $Ca_v3.2$ subunit, and that these T-channels play an important role in the excitability of developing vestibular neurones.

Methods

Isolation of primary vestibular neurones

Pregnant Swiss mice (CERJ, Le Genest, France) were killed by inhalation of CO_2 followed by cervical dislocation in accordance with French and European guidelines. The age of the E17 fetuses was determined according to the vaginal plug day (E1). The gravid uterus was collected in sterile phosphate-buffered saline (PBS, Invitrogen) supplemented with glucose (33 mM). The embryos were killed by decapitation. For each experiment about 20 vestibular ganglia were dissected and collected in sterile PBS and enzymatic dissociation was performed by treatment with 0.15% EDTA-trypsin at 37°C for 6 min. The enzymatic reaction was stopped by addition of 10% fetal calf serum (Invitrogen). The culture medium contained Neurobasal Medium supplemented with 2% B-27 (Invitrogen), 25 μM glutamate and 0.5 mM glutamine. Mechanical dissociation was performed with fire-polished Pasteur pipettes of decreasing diameters. Ganglia were carefully triturated and neurones were plated onto 35 mm culture dishes (Nunc) previously coated with 10 μg ml^{-1} polyornithine. Electrophysiological experiments were performed between 2 and 6 h after dissociation.

Ca_v3 transfection of HEK-293 cells

The culture and transfection of human embryonic kidney (HEK-293) cells were performed as previously described (Chemin *et al.* 2002*a*). The following cDNAs encoding for human α_{1G} (Monteil *et al.* 2000*a*), human $\alpha_{1I\text{-}a}$ (Monteil *et al.* 2000*b*) and human α_{1H} (Cribbs *et al.* 1998) were mixed with reporter cDNAs (GFP or CD8) using a 10 : 1 ratio. Two days after transfection, cells were re-plated at low confluence and T-currents were recorded as previously described (Chemin *et al.* 2002*a*).

Electrophysiological recordings

The patch-clamp technique was used in the whole-cell configuration to record ionic currents under voltage-clamp conditions and action potentials (APs) under current-clamp conditions using an Axopatch 200B amplifier (Axon Instruments, Foster City, CA, USA). Calcium currents were recorded using the following extracellular solution (mM): TEA-Cl 120, Hepes 10, glucose 10, and $CaCl_2$ 2, pH 7.35 (with TEA-OH). Recording pipettes (2–3 MΩ) were pulled from micro-haematocrit tubes (Modulohm I/S, Herlev, Denmark) and filled with the following solution (mM): CsCl 130, Hepes 25, glucose 10, EGTA 10, Mg-ATP 3, Na-GTP 1, pH 7.35 (with CsOH). To record APs, the extracellular solution contained (mM): NaCl 135, Hepes 10, glucose 10, $MgCl_2$ 1, KCl 5, and $CaCl_2$ 2, pH 7.35 (with NaOH). The pipette solution contained (mM): KCl 135, Hepes 10, glucose 10, NaCl 5, EGTA 5, ATP-Mg 3, GTP-Na 1, pH 7.35 (with KOH). The osmolarity of the all buffers used in this study was 310 mosmol l^{-1}. Series resistances were in the range of 5–9 MΩ corrected to 85% when necessary. The membrane capacitance could be charged with a time constant of 100 μs. No online linear leakage compensation was performed. Current signals were filtered at 10 kHz, digitized and stored. The mechanical response of T-channels was studied using a velocity-controlled perfusion system (Microlab 500B/C Series Diluter, Hamilton Company, Reno, NV, USA). Calibrated pipettes with 30 μm diameter tips were placed at a distance of 1 mm from the recorded cells to deliver extracellular medium with various velocities. Application of Ni^{2+} was performed by the successive application of various concentrations of Ni^{2+} delivered by a slow flow gravity over a 100–120 s period.

Data analysis

All experimental parameters, such as the holding and test potentials, were controlled with an IBM PC equipped with a Tecmar Labmaster analog interface (Axon Instruments). Cell stimulation, data acquisition, and analysis were performed using pCLAMP software (v6, Axon Instruments). T-current activation curves were obtained from current–voltage (I–V) relationships using the equation $g_{max} = I_{peak}/(V_m - V_R)$ where I_{peak} is the maximum current, V_m the voltage command and V_R the apparent calcium reversal potential. Since the vestibular neurones also displayed large high-voltage-activated (HVA) calcium currents (Desmadryl *et al.* 1997) we only could estimate the value of V_R at 40 mV, using an extrapolation of the ascending I–V curve ($n = 8$). Conductance values were normalized and fitted with the standard Boltzmann equation $G/G_{max} = 1/(1 + \exp((V_{1/2ac} - V_a)k_a)$ where G is the conductance at V_a potential, G_m the

maximum conductance, $V_{1/2ac}$ the midpoint of the activation curve and K_a the activation slope factor. Steady-state inactivation curves were obtained using a double-pulse protocol in which a −40 mV test pulse was preceded by a 5 s conditioning pulse at various voltages from −110 to −20 mV. Peak current at various potentials was normalized to the peak T-current amplitude measured from −110 mV and steady-state inactivation was plotted *versus* the conditioning potential. Data were fitted with a Boltzmann equation of $I/I_{max} = 1/(1 + \exp((V_i - V_{1/2inac})k_i)$ where I is the peak current at V_i potential, I_{max} the maximum current for the −110 mV conditioning pulse, $V_{1/2inac}$ the half-inactivation potential and K_i the inactivation slope factor. Time constants (τ) of activation and inactivation were best fitted with a single-exponential function of the form $I(t) = A\exp(-t/\tau)$ where A was the current peak and τ the exponential time constant. Kinetics of recovery from short inactivation were calculated with a double-exponential equation of the form $I(t) = A_1\exp(-t/\tau_1) + A_2\exp(-t/\tau_2) + C$, where A_1 and A_2 were the amplitudes of each component, τ_1 and τ_2 the time constants. The Ni^{2+} concentration–effect relationship was fitted with a Hill equation of the form $I(x) = Ax^n/(IC_{50}1^n + x^n)$ where A was the maximum response and n the Hill coefficient. Spike and after-depolarization potential (ADP) analyses were performed using pCLAMP software (v8, Axon Instruments). The AP peak values and the half-widths were determined. Rise and decay times were measured from 10% to 90% from the bottom and the top of the events. The ADP amplitudes and half-repolarization times were measured. Pooled data are given as mean ± S.D. Statistical significances were determined using Student's *t* test.

Results

Electrophysiological characteristics of the T-current in vestibular neurones

Based on the amplitude of the T-current, we previously reported that E17 primary vestibular neurones could be divided into two subpopulations (Desmadryl *et al.* 1997; Chambard *et al.* 1999). In the present study, we have focused our attention on the electrophysiological properties of the neurones with large T-current amplitudes ($I > 200$ pA in 2 mM Ca^{2+}), which represents 75% of the recorded cells (Fig. 1*A*). Calcium currents were recorded

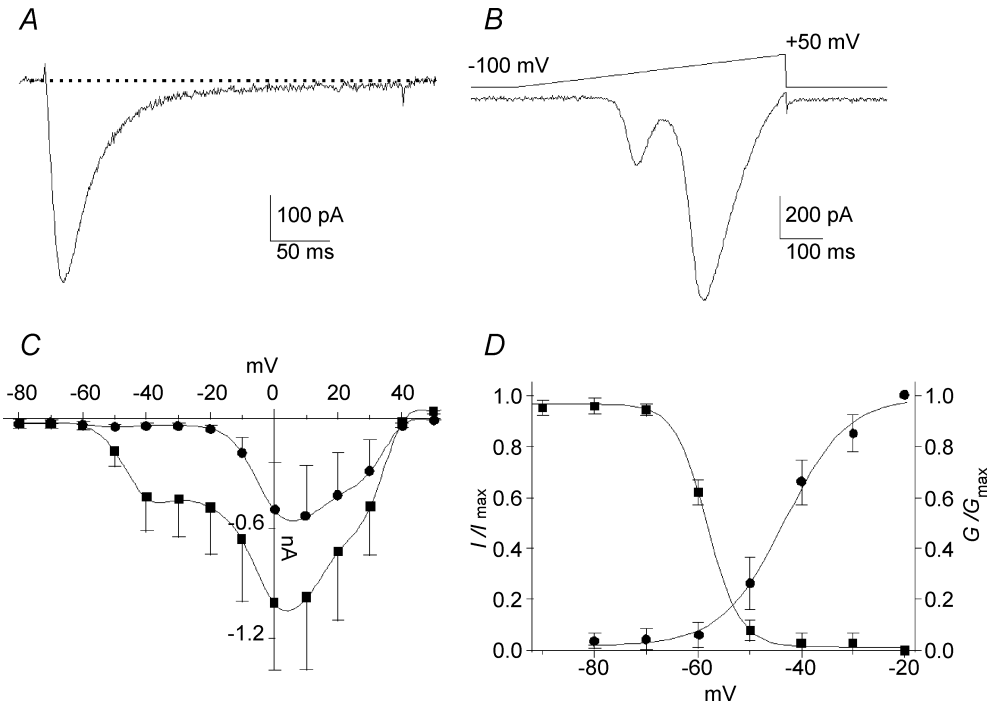

Figure 1. Calcium currents recorded in E17 primary vestibular neurones
A, typical trace of T-type current recorded in a neurone displaying large current amplitude. The current was evoked by a −35 mV pulse, at voltage eliciting the maximum amplitude determined during a voltage ramp. *B*, corresponding voltage ramp from −100 to +50 mV (640 ms duration). *C*, *I–V* relationships of global calcium current recorded from V_h −100 mV from −80 to +50 mV (■, peak current; ●, sustained current). *D*, steady-state activation (●) and inactivation (■) curves of T-current. The continuous lines represent the best-fits of the Boltzmann distribution. The overlap of activation and inactivation suggests a window current between −65 and −45 mV.

from a holding potential (V_h) of −100 mV. The average capacitance of this neurone population was 12.3 ± 3.4 pF ($n = 60$) and the mean amplitude of the T-current measured at −40 mV was 495 ± 255 pA ($n = 36$). A ramp protocol was also used to visualize LVA and HVA calcium currents (Fig. 1*B*). Using this protocol, the LVA/T-current presented a maximum peak amplitude at −38.4 ± 5.5 mV ($n = 22$). The second peak that reflected the activation of HVA currents showed a maximum at 1.8 ± 2.3 mV ($n = 24$) (Fig. 1*B*). Figure 1*C* shows *I–V* relationships of the global current, elicited by a series of 300 ms step commands from V_h −100 mV, for the peak and the sustained currents, the latter being measured between 250 and 300 ms after the pulse onset ($n = 20$). T-current activated between −60 and −50 mV, with peak current around −40 mV, while HVA activated above −20 mV. The voltage dependency of activation and inactivation properties of the T-current are illustrated in Fig. 1*D* where smooth curves correspond to Boltzmann fits with $V_{1/2ac} = -43.4 \pm 1.1$ mV (slope 6.0 ± 0.9 mV, $n = 23$) and $V_{1/2inac} = -58.2 \pm 0.3$ mV, (slope 3.1 ± 0.3 mV $n = 5$). These activation and inactivation parameters suggest a window current between −65 and −45 mV.

Activation and inactivation kinetics of the T-current displayed classical voltage-dependent properties between −50 and −20 mV (Fig. 2*A–C*). At −40 mV, the time to peak of activation was 14.8 ± 2.3 ms ($n = 18$) and the time constants for activation (τ_{ac}) and inactivation (τ_{inac}) were 10.0 ± 3.6 ms ($n = 20$) and 32.9 ± 11.1 ms ($n = 19$), respectively. To analyse T-current deactivation, cells were held at −100 mV, stepped to −40 mV for 8 ms and then hyperpolarized from −60 to −140 mV (Fig. 2*D*). T-current deactivation was best fitted by a mono-exponential function. The time constant of deactivation (τ_{deac}) was 5.28 ± 1.0 ms at −60 mV and 0.52 ± 0.09 ms at −140 mV ($n = 12$) as illustrated in Fig. 2*E*.

The recovery of T-current following short-term inactivation was investigated from V_h −100 mV using two paired-pulse protocols lasting 100 ms applied at a voltage eliciting the peak current determined during ramp stimulation. Pulses were applied with an increasing inter-pulse duration every 10 s, up to 4.5 s (Fig. 3*A*). Increased interpulse intervals were correlated with progressive increases in amplitude of the second current response. These attained maximum amplitude when the interpulse interval exceeded 3.5 s. Normalized current amplitudes calculated as the ratio of the current recorded during the second pulse to those of the conditioning pulses were plotted as function of the interpulse intervals (Fig. 3*B*). The relationships between the current recovery and the increasing interpulse interval could be fitted with one exponential with a time constant of recovery (τ_{rec}) of 571 ± 140 ms ($n = 22$). However, a two-exponential function improved the fit of the relationships with τ_{rec} of 117 ± 36 ms and 1394 ± 255 ms ($n = 22$) for, respectively, the fast and the slow components. Recovery from

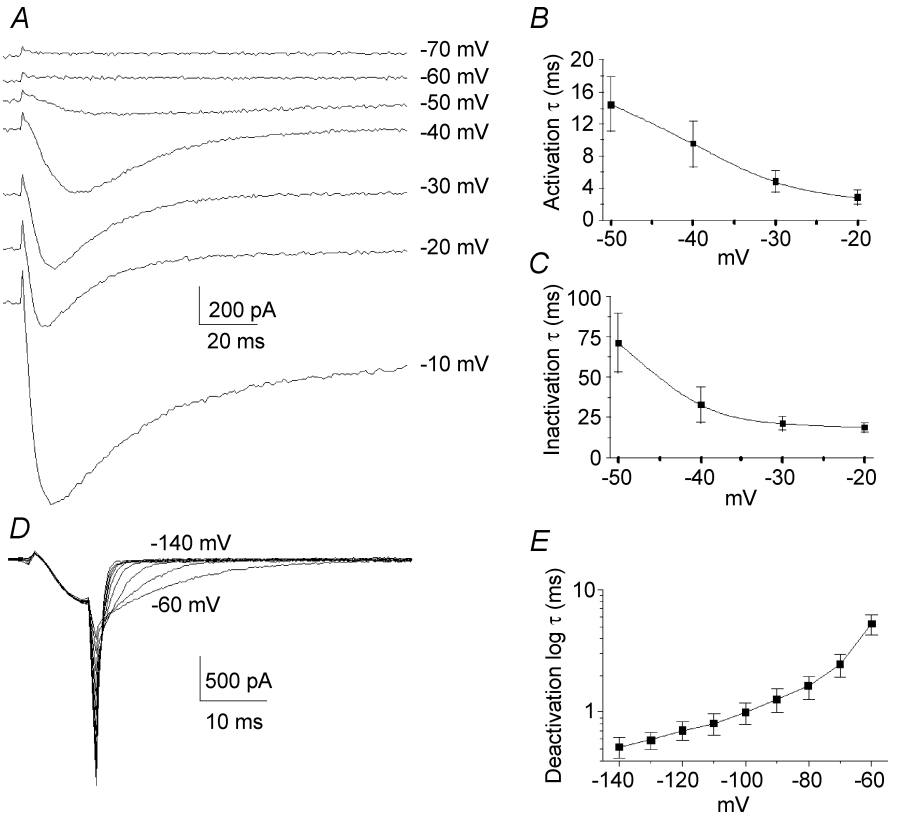

Figure 2. Activation, inactivation and deactivation properties of T-type current
A, original traces showing calcium currents at various potentials between −70 and −10 mV. The T-type current activated between −60 and −50 mV while high-voltage-activated (HVA) currents activated below −20 mV. *B*, time constants of activation of T-type current as function of the voltage. *C*, time constants of inactivation of T-type current as a function of the voltage. Both time constants of activation and inactivation were voltage dependent and present an acceleration of between −50 and −20 mV. *D*, original traces showing tail currents obtained by deactivating pulses from −140 mV to −60 mV. Pipette and cell capacitances were corrected and series resistances reduced to about 85%. *E*, plot of mean deactivating time constants of the fit of the tail currents as a function of the voltage.

inactivation for the T-current present in E17 vestibular neurones was reminiscent of that described for the $Ca_v3.2$ subunit (Chemin *et al.* 2002*a*).

T-current in vestibular neurones is affected by fast perfusion

It was reported that neuronal T-channels are affected by mechanical stimulation (Bouskila & Bostock, 1998). Because we routinely observed that a significant reduction of the T-current amplitude occurred when the primary vestibular neurones were subject to superfusion of extracellular medium, we have analysed the changes in T-current amplitude when stimulating the neurones with a fast perfusion device (see Methods). These experiments revealed that T-current amplitude in vestibular neurones was significantly reduced during perfusion (Fig. 4*A*) while HVA calcium currents were unaffected (Fig. 4*B*). Current amplitude reduction was velocity dependent and could reach up to 40% (average value $30 \pm 17\%$, $n = 24$) for the highest velocity ($2\ \mu l\ s^{-1}$). Voltage ramps applied before and after the perfusion stimulation verified the absence of shift in the activation properties (Fig. 4*B*). When the perfusion velocity was set to $1\ \mu l\ s^{-1}$, current amplitude reached a minimum in 78 ± 14 s ($n = 20$) after the beginning of the extracellular medium application. No change in either *I–V* relationships (evaluated on voltage ramps) or time to peak of activation were observed before and after the perfusion ($P > 0.2$, $n = 19$). The inactivation rates appeared to be slightly slower after perfusion ($P = 0.01$, $n = 17$). As illustrated in Fig. 4*C*, long-term recordings subsequent to the extracellular medium application ($1\ \mu l\ s^{-1}$) revealed that the recovery in current amplitude, i.e. return to the initial T-current amplitude, was obtained in about 7 min (ranging from 5 to 15 min, $n = 4$).

Since little is known about how recombinant T-channels are affected by perfusion velocity we have conducted similar experiments on HEK-293 cells that were transfected with Ca_v3 cDNAs. Recombinant T-currents were recorded before and after changes in flow velocities (Fig. 4*D–F*). Interestingly, while currents generated by the $Ca_v3.1$ (Fig. 4*D*) and $Ca_v3.3$ (Fig. 4*F*) subunits remained insensitive to such mechanical stimulus ($n = 8$ and $n = 3$, respectively), the T-current amplitude could be reduced up to 35% in cells transfected with the $Ca_v3.2$ subunit (Fig. 4*E*). On average, $Ca_v3.2$ current amplitude was significantly reduced by $24 \pm 9\%$ ($n = 11$). For perfusion velocity set to $1\ \mu l\ s^{-1}$, $Ca_v3.2$ current amplitude reached a minimum in 35 ± 10 s ($n = 6$) after the beginning of perfusion. No change in *I–V* relationships, time to peak of activation or inactivation rates were observed before and after the perfusion of recombinant Ca_v3 channels ($P > 0.2$, $n = 6$). Overall, these results indicated that the mechanical sensitivity of the T-channels in E17 vestibular neurones was similar to that of the $Ca_v3.2$ subunit as expressed in HEK-293 cells.

Sensitivity to Ni^{2+}

The analysis of sensitivity to Ni^{2+} of the T-current in primary vestibular neurones was performed under gentle superfusion of the recording chamber. A constant low rate of flow of extracellular medium was first applied to prevent any decrease in current amplitudes due to mechanical inhibition. When the T-current amplitude was stabilized in control perfusion, Ni^{2+} was applied at various concentrations. Figure 5*A* illustrates the T-current

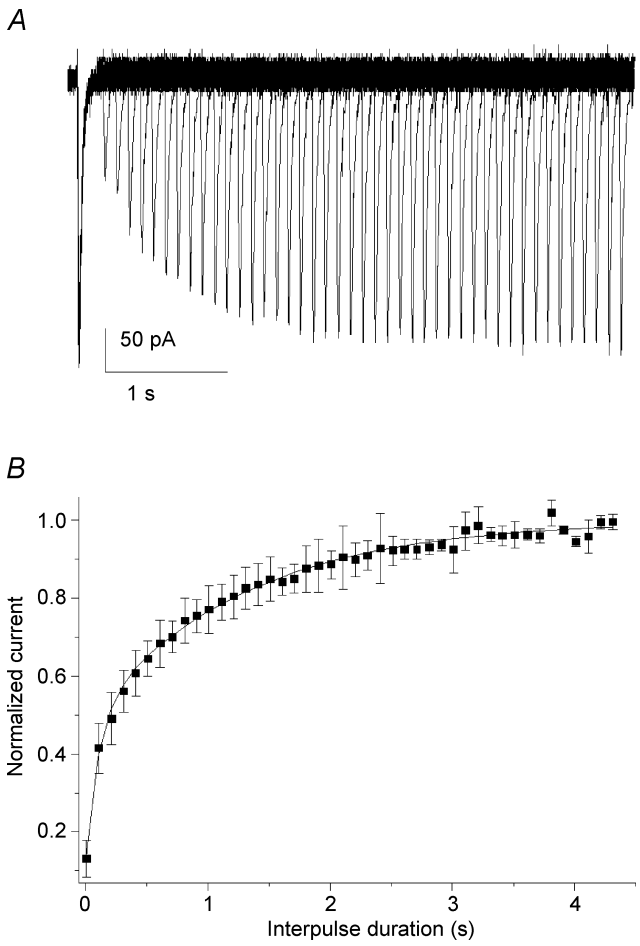

Figure 3. Time dependence of recovery following short inactivation
A, superimposed current traces obtained in an E17 vestibular neurone showing the current growth when the interval of two paired pulses (100 ms, −42 mV) increased from 0 ms up to 4.4 s (step 100 ms). *B*, plot of the mean normalized current amplitudes as a function of the interpulse interval. The relationships were fitted with two exponentials (continuous line). The time constants were 102 ± 13 and 1281 ± 41 ms, and amplitudes 0.38 ± 0.03 and 0.53 ± 0.02 ($n = 22$) for the fast and slow components, respectively.

inhibition during 10 μM Ni^{2+} application, whereas HVA calcium currents were not changed (Fig. 5*A*, inset). Since our results showed a high Ni^{2+} affinity, the reversibility analysed at 0.3 μM Ni^{2+} concentration revealed a complete reversal after wash ($n = 5$; Fig. 5*B*). Figure 5*C* shows the percentage of the T-current block as a function of the Ni^{2+} concentration from 1 nM to 10 mM. The curve fitted using a one-term Hill equation gave an IC_{50} of 13.4 μM.

Impact of T-current in AP profile

For current-clamp recordings in E17 primary vestibular neurones, APs were elicited from each neurone's resting potential (-55.0 ± 3.7 mV, $n = 34$) using a short depolarizing pulse (1.5 ms, 100–450 pA). The minimum current values required to trigger the APs and their thresholds were not significantly changed after 30 μM Ni^{2+} application (Table 1). The AP was characterized by a single Na^+-dependent spike that could be followed by an ADP (see Fig. 6*A* and *C*) or, in 30% of the neurones, by an afterhyperpolarization (AHP) (Fig. 6*D*). It is important to stress here that, in our recording conditions, no train of consecutive APs was ever seen, even with long pulses (10 s). The ADP amplitudes ranged between 8 and 33 mV above the resting potential (Table 1), with a half-repolarization time lying between 4.1 and 21.9 ms (Table 1). In 11 recorded neurones, after AP recordings, neurones were switched to voltage-clamp configuration in the presence of 300 nM TTX, 60 mM TEA and 5 mM 4-AP in the extracellular medium in order to block Na^+ and reduce K^+ conductances, as described earlier (Chabbert *et al.* 1997, 2001). In voltage-clamp conditions, when the current-clamp recordings had revealed the presence of an ADP (Fig. 6*A*) a large T-current was always observed, with a mean amplitude measured during a voltage ramp protocol of 325 ± 383 pA ($n = 5$) (Fig. 6*B*). Conversely, no large T-currents ($I < 60$ pA) were recorded in any neurones that did not exhibit ADPs ($n = 6$, data not shown), but in which AHPs were present. More importantly, gentle addition of 10 μM Ni^{2+} to the bath medium of neurones reduced the ADP component (Fig. 6*C*) in all recorded neurones ($n = 13$). The shapes of Na^+-dependent APs were not significantly different before and after 30 μM Ni^{2+} application when ADPs were recorded (Table 1; Fig. 6*C*). Application of 30 μM Ni^{2+} to neurones presenting an AHP had no effect on either the AP profiles or the post-potential component (Fig. 6*D*). Finally, when present, a significant reduction of the ADP components following APs was also obtained when a rapid perfusion of the extracellular medium was delivered to ADP-presenting neurones ($n = 8$, data not shown).

In some instances, recorded neurones could present an AP followed by Ca^{2+} spikes ($n = 5$) (Fig. 6*E*). These Ca^{2+} spikes were fully preserved when the major HVA calcium currents expressed in primary vestibular neurones, N and P/Q calcium currents (Desmadryl *et al.*

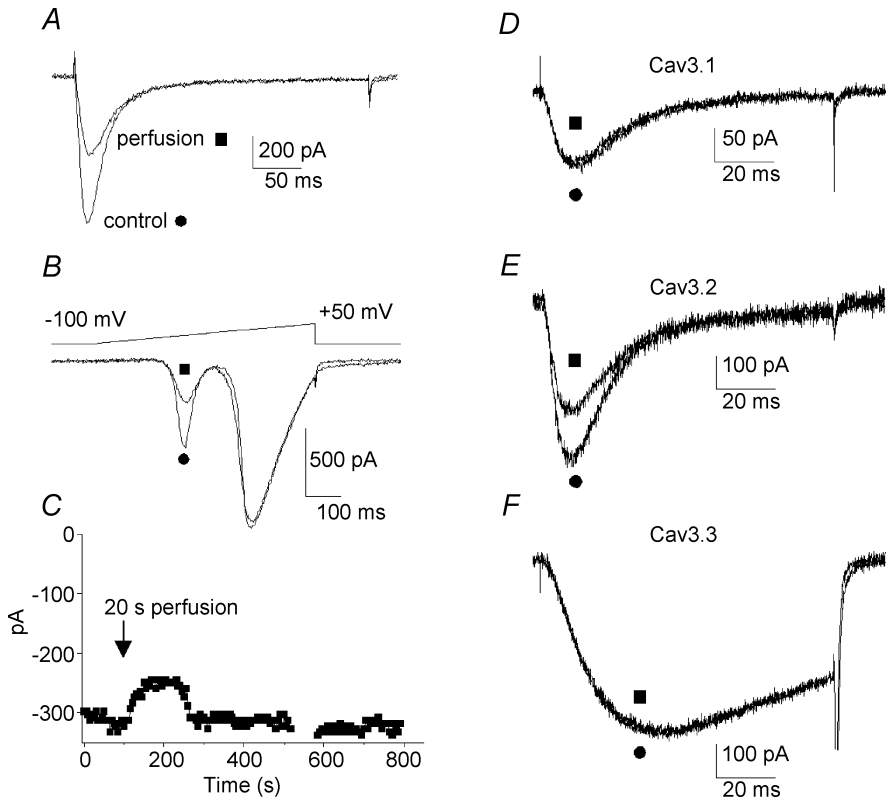

Figure 4. Mechanical responses of T-type current to the extracellular recording medium perfusion
A, original trace of T-type current recorded in E17 vestibular neurone, before (●) and after (■) application of extracellular recording medium at a velocity of 1 μl s^{-1}. *B*, corresponding voltage ramps showing the absence of shift in *I–V* relationship. Note that HVA calcium currents were not reduced. *C*, long duration recordings showing the reversibility of the extracellular medium perfusion effect on vestibular neurones. Application of recording medium (20 μl, 20 s) induced a current decrease, which reached a minimum in about 60 s and was followed by an amplitude increase to return to the initial amplitude after about 220 s. *D–F*, T-currents recorded in HEK-293 cells transfected with the different $Ca_v3/\alpha1$ T-channel subunits. Trace currents were illustrated before (●) and after (■) application of extracellular recording medium at a velocity of 1 μl s^{-1}. While $Ca_v3.1/\alpha_{1G}$ (*D*) and $Ca_v3.3/\alpha_{1I}$ (*F*) were insensitive to the perfusion, $Ca_v3.2/\alpha_{1H}$ (*E*) decreased by about 30%.

1997; Chambard *et al.* 1999), were blocked by ω-conotoxin GVIA (500 nM) and ω-agatoxin IVA (300 nM) ($n = 5$), respectively (Fig. 6*E*). When Na^+ channels were blocked (300 nM TTX) and K^+ conductances were reduced (60 mM TEA and 5 mM 4-AP) subsequent voltage-clamp recordings revealed a very large T-current (Fig. 6*F*, I ~1400 pA, for the illustrated neurone). The Ca^{2+} spikes remained stable when Na^+-dependent spikes were blocked with 300 nM TTX but were abolished by 30 μM Ni^{2+} (Fig. 6*G*).

Together, the Ni^{2+} sensitivity and mechanical sensitivity of the post-spike components in primary vestibular neurones strongly suggested that the occurrences following the AP were generated by the $Ca_v3.2$ subunit activation.

Discussion

Our results suggest that the T-channels found in embryonic primary vestibular neurones are most likely to be generated by the $Ca_v3.2/\alpha_{1H}$ subunit. Although, the present study performed on native peripheral vestibular neurones did not molecularly identify the subunit carrying the large T-current, its high sensitivity to Ni^{2+}, its mechanosensitivity (similar to that obtained with the $Ca_v3.2$ subunit transfected in HEK-293 cells), as well as its electrophysiological properties, reveal that the T-channels recorded in vestibular neurones are comparable in most aspects to cloned $Ca_v3.2$ channels (for a review see Perez-Reyes, 2003). Therefore, our results strongly support the concept that the $Ca_v3.2$ subunit is involved in the physiology of vestibular neurones. This study also demonstrates that this T-current plays a critical role in the excitability of the vestibular neurones at E17, when ontogenesis of the peripheral vestibular system takes place.

Ni^{2+} sensitivity of native and $Ca_v3.2$ T-channels

High sensitivity to Ni^{2+} is a critical distinctive feature of the recombinant Ca_v3 channels since both $Ca_v3.1$ and $Ca_v3.3$ channels present a 20-fold lower sensitivity to Ni^{2+} than $Ca_v3.2$ (Lee *et al.* 1999*b*). Our data show that the block of T-current can be observed at a concentration as low as 100 nM and was reversible. Concentration dependence of the blockade of T-current by Ni^{2+} reveals an IC_{50} of 13.4 μM comparable to the IC_{50} of 12 μM reported for cloned $Ca_v3.2$ calcium channels (Lee *et al.* 1999*b*) and is in the range of the IC_{50} of 3 μM found in sensory

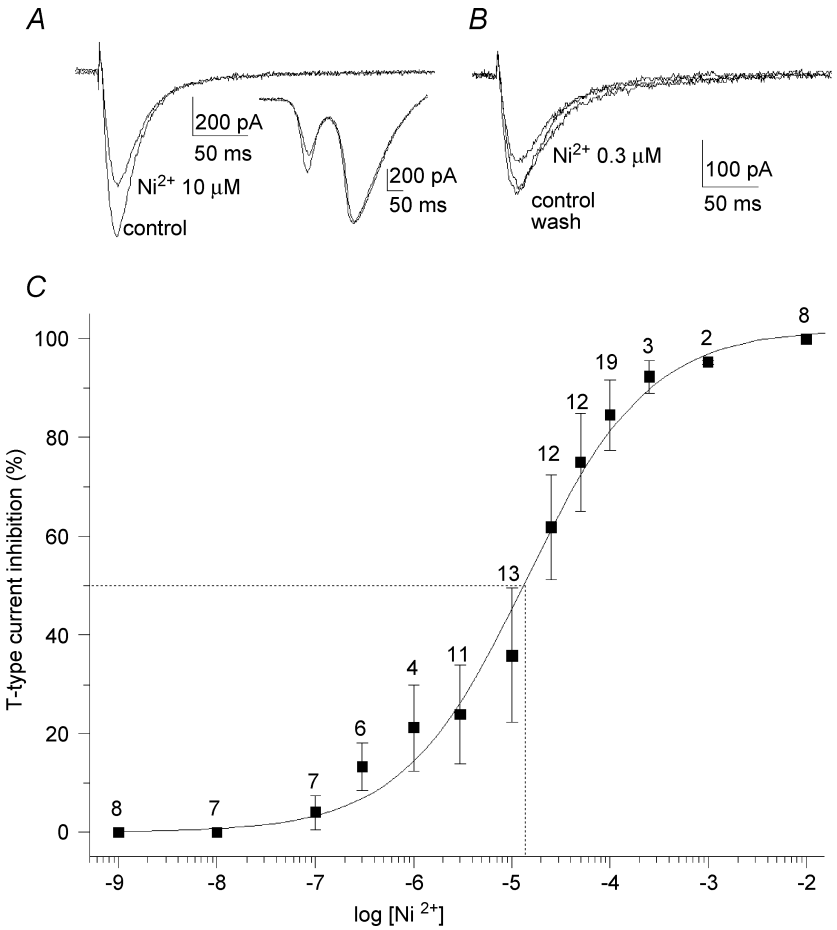

Figure 5. Effect of increasing concentration of Ni^{2+}
A, effect of 10 μM Ni^{2+} application on T-current. The HVA calcium currents were not affected (inset). *B*, reversible effect of 0.3 μM Ni^{2+} application on T-current. *C*, concentration dependence of the blockade of T-type current by Ni^{2+}. The smooth curve represents the fit of the Hill equation revealing an IC_{50} of 13.4 μM. The Hill coefficient was 0.7 ± 0.1. Dotted lines illustrate the IC_{50}. The number of observations is given above the error bars. The mechanosensitivity response is not reported in the curve.

Table 1. Action potential (AP) and afterdepolarization potential (ADP) properties

	AP		
	Control	Ni^{2+}	ADP
Trigger (pA)	248 ± 35 (6)	260 ± 52 (6)	
Threshold (mV)	−31.10 ± 2.24 (7)	−31.17 ± 2.87 (7)	
Peak value (mV)	35.3 ± 6.1 (7)	33.8 ± 8.4 (7)	
10–90% rise time (ms)	0.35 ± 0.15 (7)	0.34 ± 0.12 (7)	
10–90% decay time (ms)	0.83 ± 0.20 (7)	0.83 ± 0.18 (7)	
Half-width (ms)	1.00 ± 0.28 (7)	0.98 ± 022 (7)	
Amplitude (mV)			13.8 ± 8.6 (15)
Half-repolarization (ms)			13.3 ± 6.4 (13)

All values are given as mean ± S.D. Values in parentheses refer to number of observations. The AP properties before and after Ni^{2+} application were never significantly different (P always > 0.25).

neurones (Dubreuil *et al.* 2004). Such high sensitivity to Ni^{2+} of the T-current is a strong pharmacological argument for the claim that the $Ca_v3.2$ channel subunit carries the large T-current present in developing primary vestibular neurones.

Mechanical sensitivity of native and $Ca_v3.2$ T-channels

Another novel aspect of this study is to demonstrate the sensitivity of the native and recombinant $Ca_v3.2$ channels to the perfusion flux. In vestibular neurones short-term application of extracellular medium produces a decrease in the T-current amplitude, and in current-clamp experiments suppresses the ADP component, suggesting a direct effect of the flux on the T-channels. These responses could be reversed several minutes after the end of the perfusion flux. We also observed a comparable mechanical inhibition of T-current on recombinant $Ca_v3.2$ channels expressed in HEK-293 cells while no such modulation was found with $Ca_v3.1$ and $Ca_v3.3$ channels. Similarly, Calabrese *et al.* (2002) reported that recombinant $Ca_v3.3$ channels were insensitive to stretch stimuli. An identical mechanosensitivity of T-current induced by a stream of bath solution has been reported in rat anterior pituitary cells (Ben-Tabou *et al.* 1994) as well as in rat sensory neurones (Bouskila & Bostock, 1998). This phenomenon was also reversible within several minutes. Since the $Ca_v3.2$ isotype appears to be the principal T-channel subunit in sensory neurones (Talley *et al.* 1999), our study reconciles data obtained in vestibular (sensory) neurones and in transfected HEK-293 cells. The mechanisms by which decreases in T-current occurred during fast flow perfusion are unknown. Stream flux could induce changes in cell volume and then modulate the activity of stretch channels as reported in magnocellular neurosecretory cells (Oliet & Bourque, 1993; Bourque & Oliet, 1997). This could be mediated by a combination of force transmission through cytoskeletal and biochemical constituents (for review see Papadaki & Eskin, 1997). However, the latter hypothesis could not explain why among the three T-type Ca_v3 subunits expressed in HEK-293 cells only $Ca_v3.2$ is affected by the fast flow perfusion.

T-channels in vestibular neurones share properties of $Ca_v3.2$ subunit

The electrophysiological parameters that we have described here are complementary features to differentiate among T-type Ca_v3 subunits. The T-current in vestibular neurones showed fast activation and inactivation kinetics similar to those of $Ca_v3.1$ and $Ca_v3.2$, while the $Ca_v3.3$ current displayed activation and inactivation kinetics six times slower (Klockner *et al.* 1999; Lee *et al.* 1999*a*; McRory *et al.* 2001*a*,*b*; Chemin *et al.* 2002*a*). Therefore, a role for the $Ca_v3.3$ channels in vestibular neurones can be excluded. Deactivation kinetics is an another criterion for identifying T-channel subunits since $Ca_v3.1$ and $Ca_v3.2$ currents deactivate slowly, as compared to the $Ca_v3.3$ current (Klockner *et al.* 1999; Lee *et al.* 1999*a*; McRory *et al.* 2001*a*,*b*). Our data show that the T-current deactivates with kinetics close to those of currents induced by $Ca_v3.1$ or $Ca_v3.2$ subunits (Klockner *et al.* 1999; Kozlov *et al.* 1999; Chemin *et al.* 2002*a*). However, the deactivation rate appeared to be faster than that reported for $Ca_v3.2$ and was closer to those of the $Ca_v3.1$ subunit (Klockner *et al.* 1999; Chemin *et al.* 2002*a*). Such discrepancies could reflect differences among human and rodent T-channels as previously reported in rat brain T-channels subunits expressed in HEK-293 cells (McRory *et al.* 2001*a*,*b*). Another difference from the cloned $Ca_v3.2$ channel was the 15 mV more positive half-steady-state inactivation voltage found in primary vestibular neurones compared to that reported in cloned channels. This could depend on disparities recorded in heterologous cell expression systems and those present in between channels native

neurones that may imply specific regulations unidentified to date.

Activation, inactivation and deactivation kinetics indicate that native T-channels present in E17 vestibular neurones are likely to correspond to either $Ca_v3.1$ or $Ca_v3.2$ isotypes. Interestingly, the demonstration that recovery from short inactivation of the $Ca_v3.2$ current was a significantly slower process than that of $Ca_v3.1$ and $Ca_v3.3$ current recovery (Klockner *et al.* 1999; Chemin *et al.* 2002*a*) offers the possibility of distinguishing between $Ca_v3.1$ or $Ca_v3.2$ isotypes by an electrophysiological approach. The time constants of recovery from inactivation found in vestibular neurones were very slow and comparable to those reported in $Ca_v3.2$-transfected HEK-293 cells (Chemin *et al.* 2002*a*). However, the fits of the short inactivation recovery were improved by using two exponentials as previously reported for native T-currents in neurones (Bossu & Feltz, 1986; Takahashi *et al.* 1991), clonal pituitary cells (Herrington & Lingle, 1992) and skeletal muscle fibres (Berthier *et al.* 2002) expressing the $Ca_v3.2$ subunit. Our results indicate that the recovery following short inactivation could occur in two separate phases as reported by Berthier *et al.* (2002).

Role of T-current in AP profile

Our results suggest that T-channels could be implicated in AP repolarization components by inducing an ADP

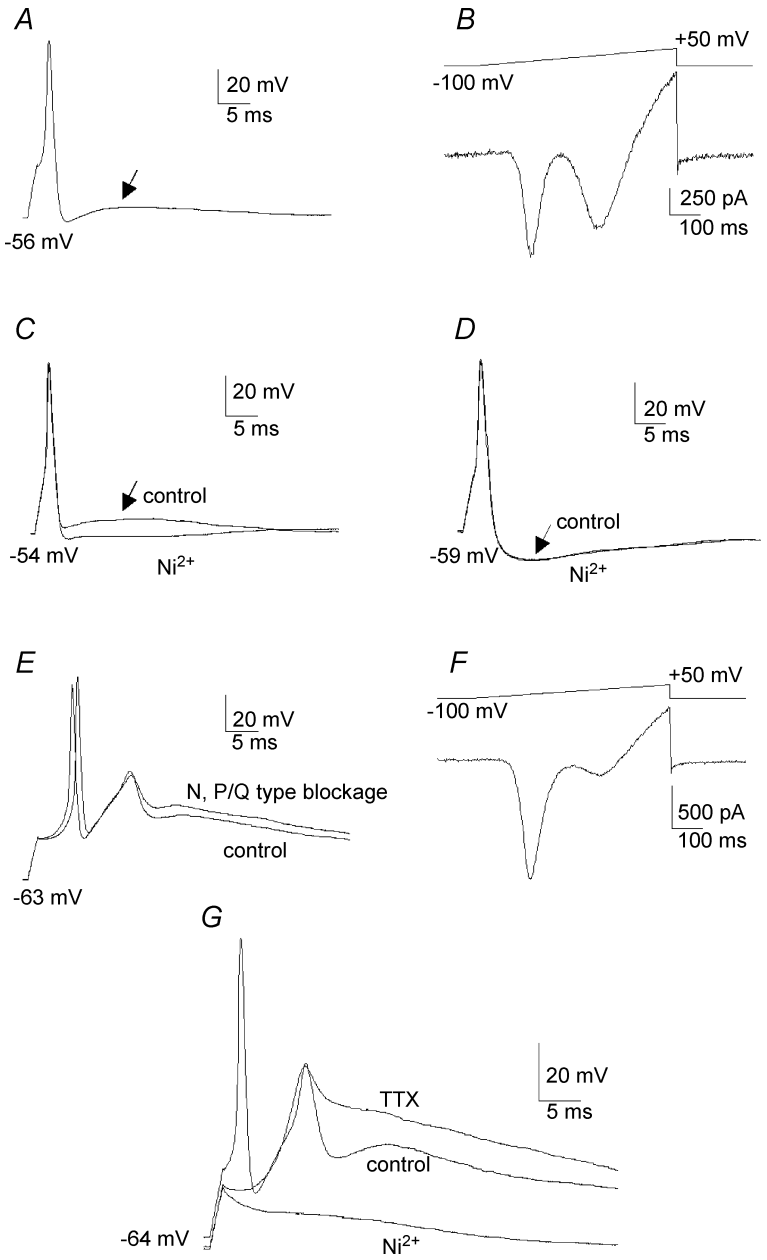

Figure 6. Implication of T-type current in AP profiles
A, action potential recorded in current clamp showing an afterdepolarization potential (ADP) (arrow) following the repolarization phase. *B*, corresponding voltage ramp recorded in the same neurone after application of TTX (300 nM), TEA (60 mM) and 4-AP (5 mM) to block the Na^+ currents and limit K^+ conductances. The voltage ramp reveals the presence of a large T-type current. It is noteworthy that the remaining K^+ conductances were presented at high voltage, mainly due to the absence of CsCl in the internal pipette medium. *C*, action potential presenting an ADP (arrow) which was blocked by the application of 10 μM Ni^{2+}. *D*, action potential presenting an afterhyperpolarization (AHP) that was insensitive to 30 μM Ni^{2+} application. *E*, Na^+-dependent action potentials followed by Ca^{2+} spikes. Application of ω-conotoxin GVIA (500 nM) and ω-agatoxin IVA (300 nM) to block N and P/Q HVA calcium channels, respectively, did not change the calcium spike amplitude. *F*, voltage ramp recorded in the same neurone showing a high amplitude T-type current after blockage of the Na^+ and K^+ conductances. In the presence of GVIA and ω-agatoxin IVA, the remaining HVA component revealed the L- and R-type calcium currents that contribute to a small fraction of the global calcium current in primary vestibular neurones. *G*, Na^+-dependent action potential followed by a Ca^{2+} spike. Application of TTX (300 nM) eliminated the Na^+-dependent action potential without affecting the calcium spike which was completely abolished by the addition of 30 μM Ni^{2+}.

or, in some instances, Ca^{2+} spikes. The involvement of the $Ca_v3.2$ subunit was further confirmed since ADP could be reduced during the application of 10 μM Ni^{2+}. At this concentration, the ADP was not totally removed since the T-current diminished by about 40%. Because the HVA calcium currents were affected by higher Ni^{2+} concentration (and probably other conductances as calcium-activated currents) we were unable to carry out concentration-dependent blockage of ADP and completely abolish this component. This contribution of T-channels in central neurones has been reported and already attributed to $Ca_v3.2$ channels since a low concentration of Ni^{2+} blocked ADP and suppressed intrinsic burst firing (Su *et al.* 2002; Dubreuil *et al.* 2004). In rat dorsal root ganglion neurones, T-current was shown to generate ADP that contributes to burst firing (Lovinger & White, 1989; Dubreuil *et al.* 2004). Moreover, in rat sensory neurones, changes in the AP repolarization phase induced by the flow of bath solution have also been reported and attributed to N-type and T-channels (Bouskila & Bostock, 1998).

Physiological significance

Based on our present data, we suggest that $Ca_v3.2$ channels are functionally expressed in E17 embryonic vestibular neurones when neuronal growth and synaptogenesis between afferents and sensory hair cells occur (Desmadryl & Sans, 1990), and therefore may play a key role in these events. The involvement of $Ca_v3.2$ in morphological differentiation has been identified in the neuroblastoma–glioma NG108-15 cell line where these channels contribute to both electrical behaviour and neuritogenesis (Chemin *et al.* 2002*b*). This $Ca_v3.2$ channel activity should contribute to a transient increase in $[Ca^{2+}]_i$ which is likely to participate in the vestibular ontogenesis by controlling axon growth and guidance, as described for embryonic spinal cord development (Gu & Spitzer, 1993; Gomez & Spitzer, 1999). Since the afferent patterns of vestibular hair cells are complex (Baird *et al.* 1988; Fernandez *et al.* 1990; Goldberg, 1991), it will therefore be relevant to investigate in detail how $Ca_v3.2$ channels modulate the ontogenesis of primary vestibular afferents and the related synaptogenesis in sensory hair cells. The role of the mechanical sensitivity of $Ca_v3.2$, which could be involved in the development of the vestibular system, should be explored further since dendritic spines are able to generate momentary contractions in relation to $[Ca^{2+}]_i$ transients evoked by action potentials (Korkotian & Segal, 2001). Further investigations could now include the exploration of the vestibular development in $Ca_v3.2$ knockout mice (Chen *et al.* 2003).

References

Anniko M (1983). Early development and maturation of the spiral ganglion. *Acta Otolaryngol* **95**, 263–276.

Baird RA, Desmadryl G, Fernandez C & Goldberg JM (1988). The vestibular nerve of the chinchilla. II. Relation between afferent response properties and peripheral innervation patterns in the semicircular canals. *J Neurophysiol* **60**, 182–203.

Ben-Tabou S, Keller E & Nussinovitch I (1994). Mechanosensitivity of voltage-gated calcium currents in rat anterior pituitary cells. *J Physiol* **476**, 29–39.

Berthier C, Monteil A, Lory P & Strube C (2002). α_{1H} mRNA in single skeletal muscle fibres accounts for T-type calcium current transient expression during fetal development in mice. *J Physiol* **539**, 681–691.

Bijlenga P, Liu JH, Espinos E, Haenggeli CA, Fischer-Lougheed J, Bader CR & Bernheim L (2000). T-type alpha 1H Ca^{2+} channels are involved in Ca^{2+} signaling during terminal differentiation (fusion) of human myoblasts. *Proc Natl Acad Sci U S A* **97**, 7627–7632.

Bossu JL & Feltz A (1986). Inactivation of the low-threshold transient calcium current in rat sensory neurones: evidence for a dual process. *J Physiol* **376**, 341–357.

Bourque CW & Oliet SH (1997). Osmoreceptors in the central nervous system. *Annu Rev Physiol* **59**, 601–619.

Bouskila Y & Bostock H (1998). Modulation of voltage-activated calcium currents by mechanical stimulation in rat sensory neurons. *J Neurophysiol* **80**, 1647–1652.

Calabrese B, Tabarean IV, Juranka P & Morris CE (2002). Mechanosensitivity of N-type calcium channel currents. *Biophys J* **83**, 2560–2574.

Chabbert C, Chambard JM, Sans A & Desmadryl G (2001). Three types of depolarization-activated potassium currents in acutely isolated mouse vestibular neurons. *J Neurophysiol* **85**, 1017–1026.

Chabbert C, Chambard JM, Valmier J, Sans A & Desmadryl G (1997). Voltage-activated sodium currents in acutely isolated mouse vestibular ganglion neurones. *Neuroreport* **8**, 1253–1256.

Chambard JM, Chabbert C, Sans A & Desmadryl G (1999). Developmental changes in low and high voltage-activated calcium currents in acutely isolated mouse vestibular neurons. *J Physiol* **518**, 141–149.

Chemin J, Monteil A, Perez-Reyes E, Bourinet E, Nargeot J & Lory P (2002*a*). Specific contribution of human T-type calcium channel isotypes (alpha$_{1G}$, alpha$_{1H}$ and alpha$_{1I}$) to neuronal excitability. *J Physiol* **540**, 3–14.

Chemin J, Nargeot J & Lory P (2002*b*). Neuronal T-type alpha 1H calcium channels induce neuritogenesis and expression of high-voltage-activated calcium channels in the NG108-15 cell line. *J Neurosci* **22**, 6856–6862.

Chen CC, Lamping KG, Nuno DW, Barresi R, Prouty SJ, Lavoie JL, Cribbs LL, England SK, Sigmund CD, Weiss RM, Williamson RA, Hill JA & Campbell KP (2003). Abnormal coronary function in mice deficient in alpha1H T-type Ca^{2+} channels. *Science* **302**, 1416–1418.

Cribbs LL, Lee JH, Yang J, Satin J, Zhang Y, Daud A, Barclay J, Williamson MP, Fox M, Rees M & Perez-Reyes E (1998). Cloning and characterization of alpha1H from human heart, a member of the T-type Ca^{2+} channel gene family. *Circ Res* **83**, 103–109.

Desarmenien MG, Clendening B & Spitzer NC (1993). In vivo development of voltage-dependent ionic currents in embryonic *Xenopus* spinal neurons. *J Neurosci* **13**, 2575–2581.

Desarmenien MG & Spitzer NC (1991). Role of calcium and protein kinase C in development of the delayed rectifier potassium current in *Xenopus* spinal neurons. *Neuron* **7**, 797–805.

Desmadryl G, Chambard JM, Valmier J & Sans A (1997). Multiple voltage-dependent calcium currents in acutely isolated mouse vestibular neurons. *Neuroscience* **78**, 511–522.

Desmadryl G & Sans A (1990). Afferent innervation patterns in crista ampullaris of the mouse during ontogenesis. *Brain Res Dev Brain Res* **52**, 183–189.

Dubreuil AS, Boukhaddaoui H, Desmadryl G, Martinez-Salgado C, Moshourab R, Lewin GR, Carroll P, Valmier J & Scamps F (2004). Role of T-type calcium current in identified d-hair mechanoreceptor neurons studied in vitro. *J Neurosci* **24**, 8480–8484.

Fernandez C, Goldberg JM & Baird RA (1990). The vestibular nerve of the chinchilla. III. Peripheral innervation patterns in the utricular macula. *J Neurophysiol* **63**, 767–780.

Goldberg JM (1991). The vestibular end organs: morphological and physiological diversity of afferents. *Curr Opin Neurobiol* **1**, 229–235.

Gomez TM & Spitzer NC (1999). In vivo regulation of axon extension and pathfinding by growth-cone calcium transients. *Nature* **397**, 350–355.

Gu X & Spitzer NC (1993). Low-threshold Ca^{2+} current and its role in spontaneous elevations of intracellular Ca^{2+} in developing *Xenopus* neurons. *J Neurosci* **13**, 4936–4948.

Gu X & Spitzer NC (1995). Distinct aspects of neuronal differentiation encoded by frequency of spontaneous Ca^{2+} transients. *Nature* **375**, 784–787.

Herrington J & Lingle CJ (1992). Kinetic and pharmacological properties of low voltage-activated Ca^{2+} current in rat clonal (GH3) pituitary cells. *J Neurophysiol* **68**, 213–232.

Klockner U, Lee JH, Cribbs LL, Daud A, Hescheler J, Pereverzev A, Perez-Reyes E & Schneider T (1999). Comparison of the Ca^{2+} currents induced by expression of three cloned alpha1 subunits, alpha1G, alpha1H and alpha1I, of low-voltage-activated T-type Ca^{2+} channels. *Eur J Neurosci* **11**, 4171–4178.

Korkotian E & Segal M (2001). Spike-associated fast contraction of dendritic spines in cultured hippocampal neurons. *Neuron* **30**, 751–758.

Kozlov AS, McKenna F, Lee JH, Cribbs LL, Perez-Reyes E, Feltz A & Lambert RC (1999). Distinct kinetics of cloned T-type Ca^{2+} channels lead to differential Ca^{2+} entry and frequency-dependence during mock action potentials. *Eur J Neurosci* **11**, 4149–4158.

Lee JH, Daud AN, Cribbs LL, Lacerda AE, Pereverzev A, Klockner U, Schneider T & Perez-Reyes E (1999*a*). Cloning and expression of a novel member of the low voltage-activated T-type calcium channel family. *J Neurosci* **19**, 1912–1921.

Lee JH, Gomora JC, Cribbs LL & Perez-Reyes E (1999*b*). Nickel block of three cloned T-type calcium channels: low concentrations selectively block alpha1H. *Biophys J* **77**, 3034–3042.

Lorenzon NM & Foehring RC (1995). Characterization of pharmacologically identified voltage-gated calcium channel currents in acutely isolated rat neocortical neurons. II. Postnatal development. *J Neurophysiol* **73**, 1443–1451.

Lovinger DM & White G (1989). Post-natal development of burst firing behavior and the low-threshold transient calcium current examined using freshly isolated neurons from rat dorsal root ganglia. *Neurosci Lett* **102**, 50–57.

McCobb DP, Best PM & Beam KG (1989). Development alters the expression of calcium currents in chick limb motoneurons. *Neuron* **2**, 1633–1643.

McRory JE, Santi CM, Hamming KS, Mezeyova J, Sutton KG, Baillie DL, Stea A & Snutch TP (2001*a*). Molecular and functional characterization of a family of rat brain T-type calcium channels. *J Biol Chem* **276**, 3999–4011.

McRory JE, Santi CM, Hamming KS, Mezeyova J, Sutton KG, Baillie DL, Stea A & Snutch TP (2001*b*). *J Biol Chem* **276**, 30571. (Erratum for *J Biol Chem* **276**, 3999–4011.)

Mariot P, Vanoverberghe K, Lalevee N, Rossier MF & Prevarskaya N (2002). Overexpression of an alpha 1H (Cav3.2) T-type calcium channel during neuroendocrine differentiation of human prostate cancer cells. *J Biol Chem* **277**, 10824–10833.

Martin-Caraballo M & Greer JJ (2001). Voltage-sensitive calcium currents and their role in regulating phrenic motoneuron electrical excitability during the perinatal period. *J Neurobiol* **46**, 231–248.

Mbiene JP, Favre D & Sans A (1988). Early innervation and differentiation of hair cells in the vestibular epithelia of mouse embryos: SEM and TEM study. *Anat Embryol (Berl)* **177**, 331–340.

Monteil A, Chemin J, Bourinet E, Mennessier G, Lory P & Nargeot J (2000*a*). Molecular and functional properties of the human alpha(1G) subunit that forms T-type calcium channels. *J Biol Chem* **275**, 6090–6100.

Monteil A, Chemin J, Leuranguer V, Altier C, Mennessier G, Bourinet E, Lory P & Nargeot J (2000*b*). Specific properties of T-type calcium channels generated by the human alpha 1I subunit. *J Biol Chem* **275**, 16530–16535.

Nordemar H (1983). Embryogenesis of the inner ear. II. The late differentiation of the mammalian crista ampullaris in vivo and in vitro. *Acta Otolaryngol* **96**, 1–8.

Oliet SH & Bourque CW (1993). Mechanosensitive channels transduce osmosensitivity in supraoptic neurons. *Nature* **364**, 341–343.

Papadaki M & Eskin SG (1997). Effects of fluid shear stress on gene regulation of vascular cells. *Biotechnol Prog* **13**, 209–221.

Perez-Reyes E (2003). Molecular physiology of low-voltage-activated t-type calcium channels. *Physiol Rev* **83**, 117–161.

Perez-Reyes E, Cribbs LL, Daud A, Lacerda AE, Barclay J, Williamson MP, Fox M, Rees M & Lee JH (1998). Molecular characterization of a neuronal low-voltage-activated T-type calcium channel. *Nature* **391**, 896–900.

Spitzer NC, Lautermilch NJ, Smith RD & Gomez TM (2000*a*). Coding of neuronal differentiation by calcium transients. *Bioessays* **22**, 811–817.

Spitzer NC, Vincent A & Lautermilch NJ (2000*b*). Differentiation of electrical excitability in motoneurons. *Brain Res Bull* **53**, 547–552.

Su H, Sochivko D, Becker A, Chen J, Jiang Y, Yaari Y & Beck H (2002). Upregulation of a T-type Ca^{2+} channel causes a long-lasting modification of neuronal firing mode after status epilepticus. *J Neurosci* **22**, 3645–3655.

Takahashi K, Ueno S & Akaike N (1991). Kinetic properties of T-type Ca^{2+} currents in isolated rat hippocampal CA1 pyramidal neurons. *J Neurophysiol* **65**, 148–155.

Talley EM, Cribbs LL, Lee JH, Daud A, Perez-Reyes E & Bayliss DA (1999). Differential distribution of three members of a gene family encoding low voltage-activated (T-type) calcium channels. *J Neurosci* **19**, 1895–1911.

Tang F, Dent EW & Kalil K (2003). Spontaneous calcium transients in developing cortical neurons regulate axon outgrowth. *J Neurosci* **23**, 927–936.

Thompson SM & Wong RK (1991). Development of calcium current subtypes in isolated rat hippocampal pyramidal cells. *J Physiol* **439**, 671–689.

Yaari Y, Hamon B & Lux HD (1987). Development of two types of calcium channels in cultured mammalian hippocampal neurons. *Science* **235**, 680–682.

Acknowledgements

The authors thank G. Dayanithi for critically reviewing the manuscript. We acknowledge Professor A. Sans director of the INSERM U432 laboratory where our first investigations were realized. We thank M. Breisse and D. Greuet for their assistance in the technical preparations. The work was supported by CNES grants 8529/00 and793/01.